

# Multiphysics modeling and design of Galfenol-based unimorph harvesters

Zhangxian Deng, Marcelo J. Dapino

NSF I/UCRC on Smart Vehicle Concepts, Department of Mechanical and Aerospace Engineering, The Ohio State University, Columbus, OH, USA, 43210

## ABSTRACT

Iron-gallium alloys, known as Galfenol, are a class of magnetostrictive materials that convert mechanical energy to magnetic energy and vice versa. Galfenol devices especially unimorph consisting of a Galfenol beam bonded to a passive substrate, have great potential in energy harvesting applications, but advanced multiphysics models are lacking for these smart devices. This study presents a comprehensive finite element model for Galfenol unimorph harvesters which incorporates magnetic, mechanical, and electrical dynamics. Experiments considering impulsive tip excitations under purely resistive or resistive-capacitive electrical loads are conducted to validate the proposed model. The energy conversion efficiency and peak power density of a unimorph beam with a natural frequency of 139.5 Hz are analyzed experimentally. The maximum energy conversion efficiency is 5.93% when a 74  $\Omega$  resistor and a 2  $\mu\text{F}$  capacitor are connected in parallel to the pickup coil in parallel. The maximum power density observed in experiments is 10.72 mW/cm<sup>3</sup> when load resistance is 74  $\Omega$ . This performance may be optimized in the future utilizing the proposed finite element model.

**Keywords:** Galfenol, energy harvester, unimorph, COMSOL Multiphysics

## 1. INTRODUCTION

Magnetostrictive iron-gallium alloys (Galfenol) are a class of smart materials that exhibit moderate magnetostriction (around 400 ppm) and magnetization (1200 kA/m). The material has a relatively high tensile strength compared to other smart materials such as Terfenol-D and piezoelectric materials. Hence, it is robust even when subjected to combined loading.

With the development of integrated circuits, recent embedded or wireless sensors have experienced a reduction in size and energy consumption. Built-in power sources for those devices eliminates the need for frequent battery replacement. Vibration-based energy harvesters are able to scavenge structural vibration and convert it to useful electrical energy. They improve system efficiency and reduce noise.<sup>1</sup> Galfenol exhibits strong magneto-mechanical coupling, and thus it is attractive for implementation in energy harvester designs. Staley and Flatau<sup>2</sup> investigated the energy harvesting properties of Galfenol under various bias conditions. Ueno and Yamada<sup>3</sup> experimentally analyzed a bimorph harvester that consists of two Galfenol layers bonded together and evaluated its energy conversion efficiency by applying impulsive tip excitations. Berbyuk<sup>4</sup> developed a Galfenol-based energy harvester in axial mode and achieved 338 mW/cm<sup>3</sup> power density. Deng and Dapino<sup>5</sup> conducted experiments on Galfenol unimorph energy harvesters considering various design parameters such as load resistance, beam thickness ratio, and bias magnetic field strength.

Efficient and accurate system-level models are necessary for Galfenol device design and optimization. Yoo et al.<sup>6</sup> presented a lumped parameter model for unimorph energy harvesters based on linearized

Further author information: (Send correspondence to M.J.D)  
Z.D.: E-mail: deng.92@osu.edu, Telephone: 1-614-886-4687  
M.J.D.: E-mail: dapino.1@osu.edu, Telephone: 1-614-688-3689

Industrial and Commercial Applications of Smart Structures Technologies 2015,  
edited by Kevin M. Farinholt, Steven F. Griffin, Proc. of SPIE Vol. 9433, 94330B  
© 2015 SPIE · CCC code: 0277-786X/15/\$18 · doi: 10.1117/12.2085550

magnetomechanical equations. Zhao and Lord<sup>7</sup> included eddy currents and electrical dynamics as part of linearized piezomagnetic equations and theoretically quantified the maximum output power of Galfenol-based energy harvesters at high frequencies. However, linear equations are not accurate enough to describe Galfenol in nonlinear regimes that include material anisotropy, hysteresis, and saturation.

Energy based constitutive models for magnetostrictive materials have been developed<sup>8,9</sup> which stimulated the development of finite element models for Galfenol-based devices. Shu et al.<sup>10</sup> combined a discrete energy averaged model with 2D Euler beam theory and created a finite element model for Galfenol unimorphs driven under constant magnetic fields. Chakrabarti and Dapino<sup>11</sup> developed a 3D fully nonlinear anhyseretic finite element model for a Galfenol unimorph actuator. Deng and Dapino<sup>12</sup> later added material hysteresis to this model. To improve model efficiency, Rezaeealam et al.<sup>13</sup> presented a 2D finite element model in which Galfenol nonlinearities were described through calculated nonlinear lookup tables. Deng and Dapino<sup>5</sup> utilized the discrete energy averaged model to generate the lookup tables and proposed a systematic optimization procedure for Galfenol unimorph harvesters.

In this study, a unimorph with a natural frequency of 139.5 Hz is tested by applying impulsive tip deflection under purely resistive or resistive-capacitive electrical loading. The maximum energy conversion efficiency observed in experiments is 5.93% when the electrical load is composed of a 74  $\Omega$  resistor and 2  $\mu$ F capacitor connected in parallel. The maximum power density is 10.72 mW/cm<sup>3</sup> at a 74  $\Omega$  load resistance. A simplified 2D FEA model, incorporating mechanical, magnetic, and electrical dynamics, is developed based on calculated nonlinear lookup tables. The proposed model is able to accurately describe the system for both types of electrical loads.

## 2. THEORY

### 2.1 Thin glue layer

Figure 1 shows the 2D geometry of a unimorph harvester. A previous FE model for Galfenol unimorphs assumes that the Galfenol layer is rigidly connected to the stainless steel substrate.<sup>5</sup> In practice, both layers are bonded together using strain gauge glue (M-bond 200) with a modulus of about 9 MPa. This thin glue layer ( $\approx 0.0254$  mm) reduces the overall stiffness of the beam thus it must be taken into consideration. Directly modeling the glue layer as a 3D subdomain requires an extremely fine mesh which greatly reduces computational efficiency. This study decouples the geometric continuity between the Galfenol and substrate layers, and connects them by an elastic force  $\mathbf{F}_e$  and a viscous force  $\mathbf{F}_v$ ,

$$\begin{aligned}\mathbf{F}_e &= \mathbf{k}\Delta\mathbf{u}, \\ \mathbf{F}_v &= \mathbf{c}\Delta\dot{\mathbf{u}},\end{aligned}\tag{1}$$

where  $\Delta\mathbf{u}$  is the relative displacement between the two layers. The terms  $\mathbf{k}$  and  $\mathbf{c}$  are the stiffness and the damping coefficient of the glue layer, respectively. The force on the glue layer  $\sigma_g$  satisfies

$$\sigma_g \cdot \mathbf{n} = -\mathbf{F}_e - \mathbf{F}_v,\tag{2}$$

where  $\mathbf{n}$  is the unit norm vector of the glue layer.

### 2.2 Electrical dynamics and impedance matching

It has been shown that the output power of a unimorph harvester depends on load impedance,<sup>5,14</sup> but none of those studies provides an accurate and efficient FE tool that fully couples the magnetic, mechanical, and electrical dynamics. COMSOL Multiphysics recently developed a powerful interface that is able to connect SPICE netlists to magnetic subdomains. This study considers a resistor  $R_L$  and a capacitor  $C$  connecting in parallel with the pickup coil, as shown in Figure 2. The input voltage  $V$  is

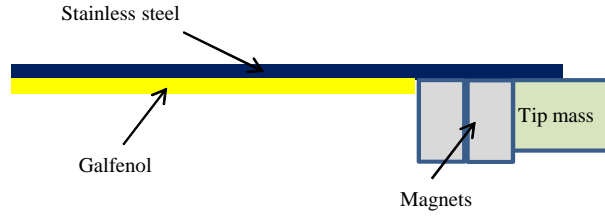


Figure 1. Geometry of unimorph harvester in COMSOL Multiphysics.

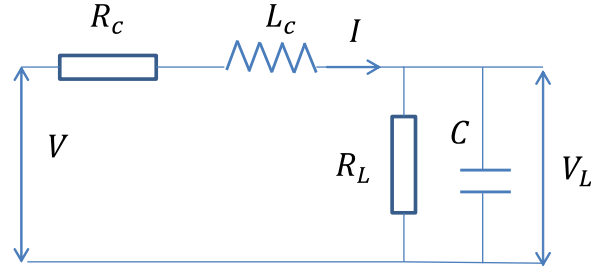


Figure 2. Equivalent circuit for the pickup coil and the electrical load.

calculated from the pickup coil subdomains using Faraday's law. The induced current  $I$  flows through the coil and generates magnetic field along the length of the beam.

Assuming that the input voltage  $V$  is sinusoidal and its angular frequency is  $\omega$ , the average output power on the resistor is

$$\begin{aligned}\bar{P} &= \frac{1}{T} \int_0^T \frac{V(t)}{R_L} dt \\ &= \frac{V_{amp}}{2} \frac{1}{(L_c^2 C^2 \omega^4 + R_c^2 C^2 \omega^2 - 2L_c C \omega^2 + 1)R_L + (L_c^2 \omega^2 + R_c^2)/R_L + 2R_c},\end{aligned}\quad (3)$$

where  $V_{amp}$  is the amplitude of  $V(t)$ ,  $L_c$  is the coil inductance,  $R_c$  is the coil resistance, and  $T$  is the period of  $V$ . The maximum average output power is

$$\max(\bar{P}) = \frac{V_{amp}^2}{8R_c}, \quad (4)$$

when

$$C = \frac{L_c}{L_c^2 \omega^2 + R_c^2} \text{ and } R_L = \frac{R_c^2 + L_c^2 \omega^2}{R_c}. \quad (5)$$

When the capacitor is disconnected ( $C = 0$ ), the maximum average output power is

$$\max(\bar{P}|_{C=0}) = \frac{V_{amp}^2}{4} \frac{1}{R_c + \sqrt{R_c^2 + L_c^2 \omega^2}} \quad (6)$$

where  $R_L = \sqrt{R_c^2 + L_c^2 \omega^2}$ . Since  $L_c > 0$ ,

$$\max(\bar{P}|_{C=0}) < \frac{V_{amp}^2}{4} \frac{1}{2R_c} = \max(\bar{P}). \quad (7)$$

Equation (7) shows that the capacitor compensates for the impedance due to the coil inductance, and thus helps to increase the output power.

### 3. EXPERIMENT AND MODELING

#### 3.1 Experimental setup

Figure 3 shows the experimental setup that is used to evaluate the performance of unimorph harvester under impulsive tip deflection. One of the design parameters that affects the energy harvesting capacity is the beam thickness ratio, which is defined as the thickness of the substrate layer over the thickness of the Galfenol. Previous experiments and parametric studies have shown that a beam with a thickness ratio of 2 generates maximum output power.<sup>5</sup> Hence, experiments in this study focus on this thickness ratio only.

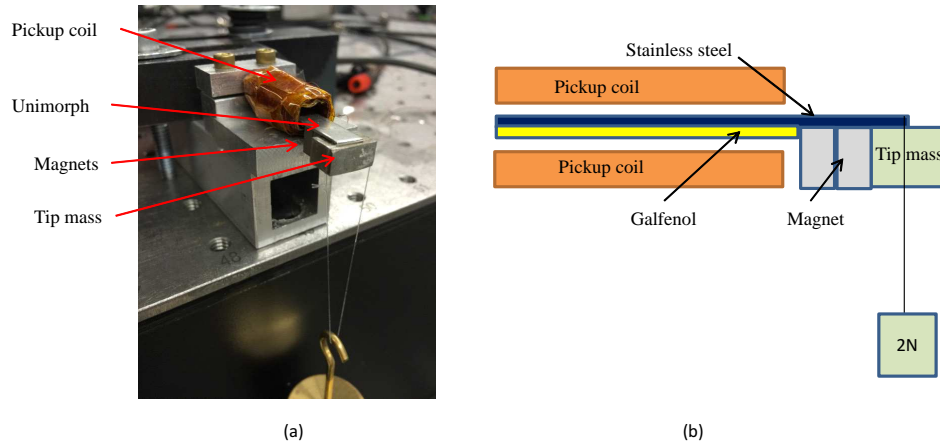


Figure 3. (a) Experiment setup; (b) cross-sectional view of the unimorph harvester.

As shown in Figure 3, a 38.1 mm×6.35 mm×0.381 mm polycrystalline Galfenol (with 18.4% gallium) beam manufactured by Etrema Products, Inc. is bonded to a 316 stainless steel beam (38.1 mm×6.35 mm×0.762 mm). About 11.43 mm of the unimorph beam is constrained inside the aluminum fixture, so the effective length of the Galfenol layer is 26.67 mm. A 3.68 g stainless steel tip mass is glued on the beam tip, and two permanent magnets with a remanent flux of about 1.1 T are attached to generate a bias magnetic field. A 1 inch long, 1100 turns pickup coil made of AWG 36 copper wire with a resistance of 56.2  $\Omega$  is wound around the unimorph beam. The tip deflection is measured by a Keyence LK-G32 laser position sensor. A resistance decade box ( $\pm 1\%$  accuracy) and a capacitance decade box ( $\pm 5\%$  accuracy) are used to adjust the load impedance. Voltage on the resistor and the tip deflection signals are sent to a Quattro data acquisition system at a 5.12 kHz sampling rate.

To quantify the performance of the unimorph harvester, the following metrics are implemented:

1. Peak power and peak power density

The peak power  $P_{peak}$  and the peak power density  $D_{peak}$  have been widely utilized in previous energy harvester studies<sup>3</sup>

$$P_{peak} = \frac{V_{max}^2}{R_L}, \quad D_{peak} = \frac{P_{peak}}{V_g}, \quad (8)$$

where  $V_{max}$  is the maximum voltage on the resistor and  $V_g$  is the volume of the Galfenol layer.

2. Energy conversion efficiency

The total output electrical energy on the resistor is  $E_{out} = \int_0^\infty V_L^2(t)/R_L dt$ . The mechanical energy input  $E_{in} = 0.5F_{tip}D_{tip}$ , where  $F_{tip}$  is the initial tip force and  $D_{tip}$  is the initial tip deflection. The energy conversion efficiency is

$$\eta = \frac{E_{out}}{E_{in}}. \quad (9)$$

### 3.2 Open circuit

A 2 N mass is hung on the tip of the unimorph beam, as shown in Figure 3. The unimorph starts an impulsive response as soon as the fishing wire is cut. The tip deflection  $D(t)$  decays exponentially as

$$D(t) = D_{tip}e^{-2\pi f_r \xi t} \cos(2\pi \sqrt{1 - \xi^2} f_r t), \quad (10)$$

where  $\xi$  is the damping ratio and  $f_r$  is the fundamental frequency. Figure 4 shows that Equation (10) can accurately describe the decay of the tip displacement with  $f_r = 139.5$  Hz and  $\xi = 0.0045$ . Since no resistors are connected to the pickup coil, the mechanical energy is dissipated through structural damping and Galfenol hysteresis loss. The damping ratio is simulated through Rayleigh damping<sup>5,10</sup> in the finite element model.

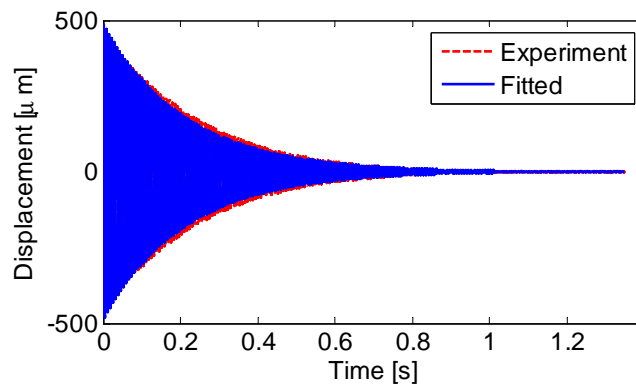


Figure 4. Comparison of the experimental impulsive response (open circuit) and model calculation for the tip deflection.

The backward differentiation formula (BDF) method used in previous studies<sup>10,11,15</sup> introduces numerical damping to filter out high frequency components, and thus improves model convergence. However, an ideal impulsive input signal, which has a wide frequency span in its spectrum, excites almost all modes of the beam. Hence, the model will have significant error if the high frequency modes are eliminated by the BDF method. This study implements the BDF –  $\alpha$  method that is able to control the numerical damping. Figures 5 and 6 compare the impulsive response of the tip deflection  $D(t)$  and voltage  $V_L$ . The proposed finite element model is able to accurately describe the dynamic response for the open circuit conditions.

### 3.3 Purely resistive loading

Equation (6) shows that the output power and output power density depend on the load resistance connected to the pickup coil. Figures 7(a) and 7(b) present the experimental results of the peak output power  $P_{peak}$  and the peak output power density  $D_{peak}$  with respect to different resistive loads. The maximum  $P_{peak}$  and  $D_{peak}$  are 0.628 mW and 10.22 mW/cm<sup>3</sup>, respectively, when the load resistance is  $R_L = 74 \Omega$ .

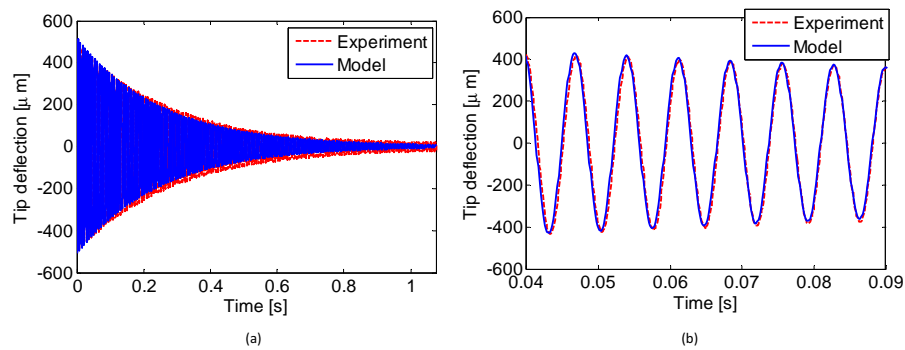


Figure 5. Open circuit response. (a) Impulsive response (tip deflection) of the unimorph; (b) zoomed in view of the tip deflection (0.04-0.09 s).

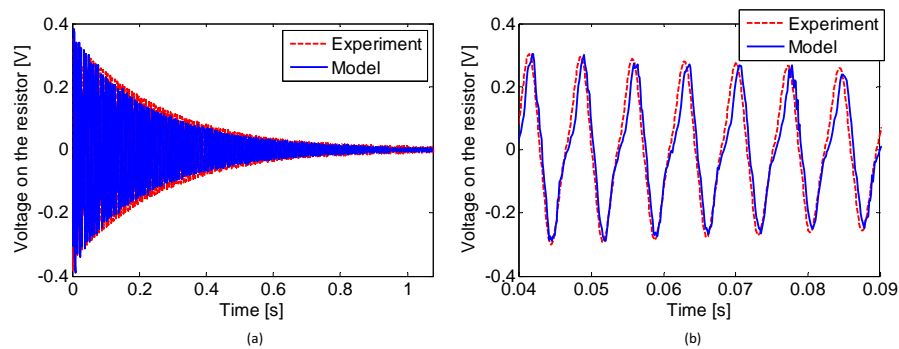


Figure 6. Open circuit response. (a) Impulsive response of  $V_L$  when no resistor is connected; (b) zoomed in view of the output voltage (0.04-0.09 s).

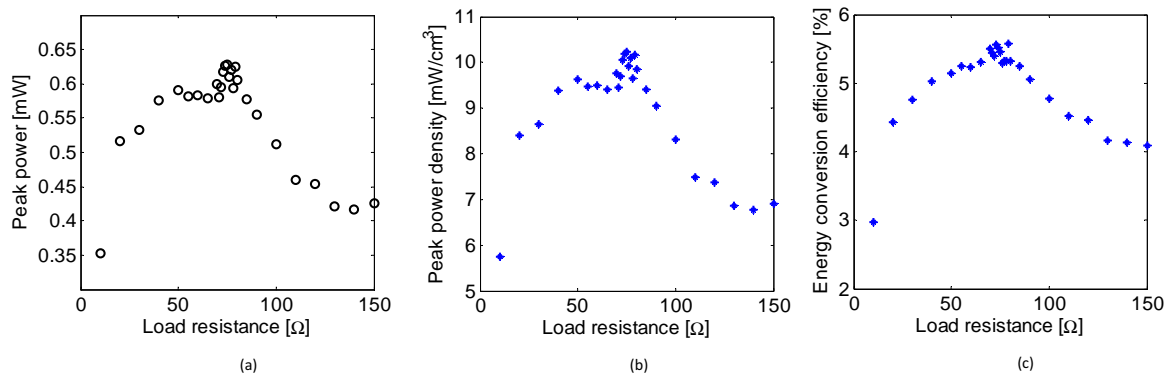


Figure 7. Resistive electrical load. (a) Peak output power  $P_{peak}$ ; (b) peak output power density  $D_{peak}$ ; (c) energy conversion efficiency  $\eta$ .

Figure 7(c) shows the energy conversion efficiency  $\eta$ . The maximum  $\eta = 5.52\%$  when  $R_L = 74 \Omega$ . The finite element model is able to accurately describe the dynamic response for purely resistive electrical load (Figures 8 and 9).

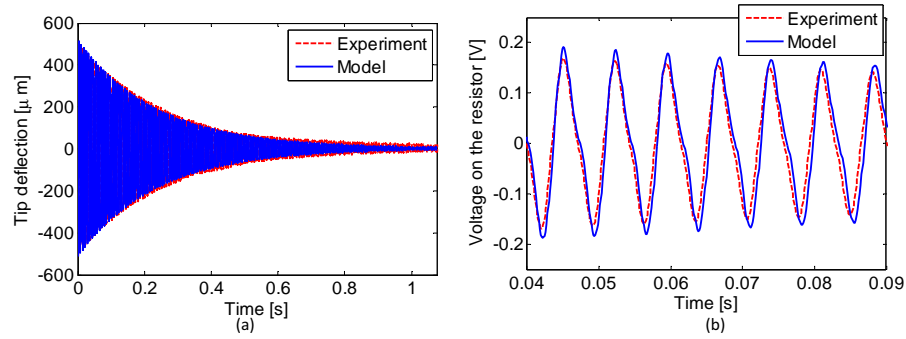


Figure 8. Load resistance  $R_L = 74 \Omega$ . (a) Impulsive response (tip deflection) of the unimorph; (b) zoomed in view of the tip deflection (0.04-0.09 s).

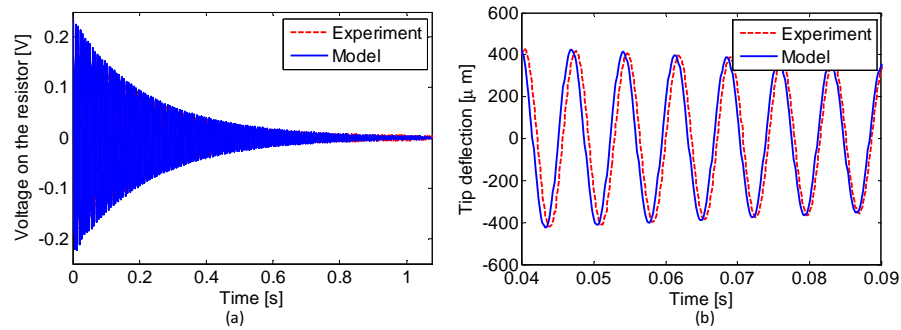


Figure 9. Load resistance  $R_L = 74 \Omega$ . (a) Impulsive response of  $V_L$  when  $R_L = 74 \Omega$ ; (b) zoomed in view of the output voltage (0.04-0.09 s).

### 3.4 Resistive-capacitive loading

Equation (5) proves that the output power of the unimorph beam harvester can be improved by connecting a capacitor in parallel to the resistive load. Experimental results show that  $P_{peak}$  and  $D_{peak}$  values decrease with respect to the  $C$  values (Figure 10(a) and 10(b)), but  $\eta$  is improved by at most 7.4% (Figure 10(c)). The maximum  $\eta = 5.93\%$  when a  $2 \mu\text{F}$  capacitor is attached to the  $74 \Omega$  resistive load.

Figures 11 and 12 show that the finite element model can accurately describe the dynamic response of the unimorph under resistive-capacitive loading conditions.

## 4. DISCUSSION

Multiple performance metrics, including energy conversion efficiency  $\eta$ , output power density, and output power, have been used to evaluate the performance of Galfenol based energy harvesters.<sup>3,5,6</sup> Depending

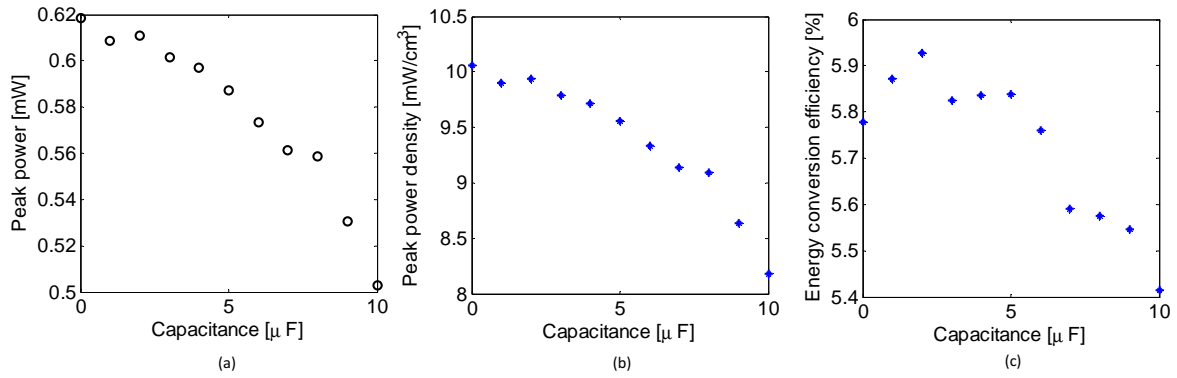


Figure 10. Capacitive electrical load and  $R_L = 74 \Omega$ . (a) Peak output power  $P_{peak}$ ; (b) Peak output power density  $D_{peak}$ ; (c) Energy conversion efficiency  $\eta$ .

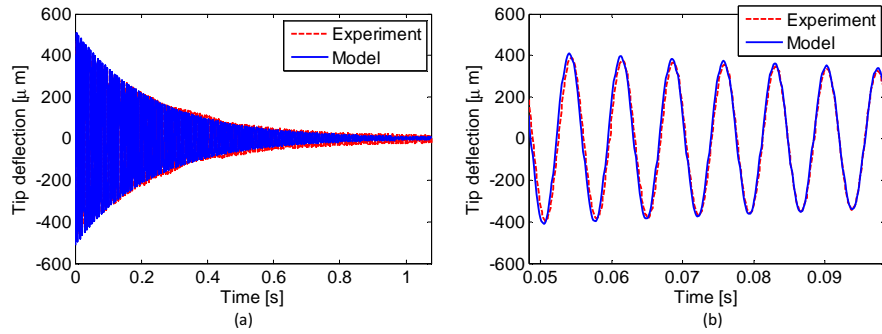


Figure 11. Impulsive response when  $R_L = 74 \Omega$  and  $C = 2 \mu\text{F}$ . (a) Impulsive response (tip deflection) of the unimorph; (b) zoomed in view of the tip deflection (0.04-0.09 s).

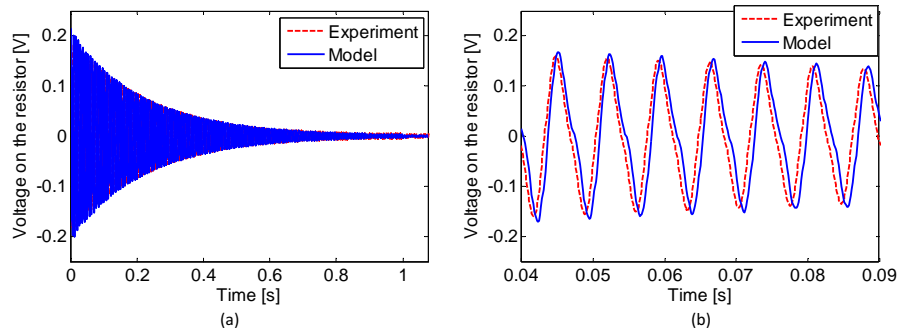


Figure 12. Impulsive response when  $R_L = 74 \Omega$  and  $C = 2 \mu\text{F}$ . (a) Impulsive response (voltage on the resistor) of the unimorph; (b) zoomed in view of the output voltage (0.04-0.09 s).



on the details of a given application, different metrics need to be selected. In this study,  $\eta$  quantifies system efficiency thus it is the major metric to be considered. Ueno and Yamada<sup>3</sup> reported a maximum energy conversion efficiency  $\eta = 16\%$  for a Galfenol bimorph subjected to impulsive tip excitations. The natural frequency  $f_r$  of their beam was 395 Hz. The maximum  $\eta$  observed in this study is 5.93%, and the unimorph has a natural frequency of 139.5 Hz. However, Ueno and Yamada<sup>3</sup> showed that  $\eta$  is nearly proportional to  $f_r$ ; thus, a unimorph harvester with a higher natural frequency is expected to achieve higher efficiency. In particular, preliminary modeling results show that  $\eta$  is about 17% when the natural frequency of the unimorph is increased to 395 Hz. Consequently, magnetostrictive energy harvesters can be accurately compared only if  $\eta$  is normalized such that the effect of input force and  $f_r$  are compensated for; this topic will be the focus of a future study.

## 5. SUMMARY AND FUTURE WORK

This study experimentally quantified the performance of a Galfenol-based unimorph energy harvester with a natural frequency of 139.5 Hz in terms of peak output power  $P_{peak}$ , peak output power density  $D_{peak}$ , and energy conversion efficiency  $\eta$ . When resistive loads were connected to the pickup coil, the maximum  $P_{peak}$ ,  $D_{peak}$ , and  $\eta$  (at  $R_L = 74 \Omega$ ) are 0.628 mW, 10.22 mW/cm<sup>3</sup>, and 5.52%, respectively. Connecting a capacitor in parallel to the resistive load reduced  $P_{peak}$  and  $D_{peak}$ , but improved the overall energy conversion efficiency. The value of  $\eta$  was increased from 5.52% to 5.93% (by 7.4%) when a 2  $\mu$ F capacitor was connected. A 2D finite element model, considering mechanical, magnetic, and electrical dynamics of the unimorph system, was proposed and validated in this study. The modeled impulsive response proved the accuracy of the model under purely resistive and resistive-capacitive electrical loads. Based on the proposed model, a parametric study targeting maximizing  $\eta$  will be developed in the future. The unimorph harvester will be placed on top of an electrical shaker and its performance under sinusoidal and broadband excitation will be quantified.

## ACKNOWLEDGMENTS

We wish to acknowledge the member organizations of the Smart Vehicle Concepts Center, a National Science Foundation Industry/University Cooperative Research Center ([www.SmartVehicleCenter.org](http://www.SmartVehicleCenter.org)) established under NSF Grant IIP-1238286.

## REFERENCES

1. Z. Deng V. Asnani, and M. J. Dapino, "Magnetostrictive vibration damper and energy harvester for rotating machinery," in *SPIE Smart Structures and Material & Nondestructive Evaluation and Health Monitoring* (under review), International Society for Optics and Photonics, 2015.
2. M. E. Staley and A. B. Flatau, "Characterization of energy harvesting potential of Terfenol-D and Galfenol," in *Smart Structures and Materials*, pp. 630–640, International Society for Optics and Photonics, 2005.
3. T. Ueno and S. Yamada, "Performance of energy harvester using iron–gallium alloy in free vibration," *Magnetics, IEEE Transactions on* **47**(10), pp. 2407–2409, 2011.
4. V. Berbyuk, "Vibration energy harvesting using Galfenol-based transducer," in *SPIE Smart Structures and Materials+ Nondestructive Evaluation and Health Monitoring*, pp. 86881F–86881F, International Society for Optics and Photonics, 2013.
5. Z. Deng and M. J. Dapino, "Modeling and design of Galfenol unimorph energy harvester," in *SPIE Smart Structures and Material & Nondestructive Evaluation and Health Monitoring*, pp. 90572A–90572A, International Society for Optics and Photonics, 2014.
6. J. H. Yoo and A. B. Flatau, "A bending-mode Galfenol electric power harvester," *Journal of Intelligent Material Systems and Structures* **23**(6), pp. 647–654, 2012.

7. X. Zhao and D. Lord, "Application of the villari effect to electric power harvesting," *Journal of Applied Physics* **99**(8), p. 08M703, 2006.
8. P. Evans and M. Dapino, "Efficient magnetic hysteresis model for field and stress application in magnetostrictive Galfenol," *Journal of Applied Physics* **107**(6), pp. 063906–063906, 2010.
9. W. Armstrong, "An incremental theory of magneto-elastic hysteresis in pseudo-cubic ferro-magnetostrictive alloys," *Journal of Magnetism and Magnetic Materials* **263**(1), pp. 208–218, 2003.
10. L. Shu, M. J. Dapino, P. G. Evans, D. Chen, and Q. Lu, "Optimization and dynamic modeling of Galfenol unimorphs," *Journal of Intelligent Material Systems and Structures* **22**(8), pp. 781–793, 2011.
11. S. Chakrabarti and M. J. Dapino, "Nonlinear finite element model for 3D Galfenol systems," *Smart Materials and Structures* **20**(10), p. 105034, 2011.
12. Z. Deng and M. J. Dapino, "Characterization and finite element modeling of Galfenol minor flux density loops," *Journal of Intelligent Material Systems and Structures*, p. 1045389X14521703, 2014.
13. B. Rezaeealam, T. Ueno, and S. Yamada, "Finite element analysis of Galfenol unimorph vibration energy harvester," *Magnetics, IEEE Transactions on* **48**(11), pp. 3977–3980, 2012.
14. J. Yoo, A. Murray, and A. B. Flatau, "Evaluation of magnetostrictive shunt damper performance using iron (Fe)-gallium (Ga) alloy," in *SPIE Smart Structures and Materials & Nondestructive Evaluation and Health Monitoring*, pp. 90573I–90573I, International Society for Optics and Photonics, 2014.
15. L. Shu, L. M. Headings, M. J. Dapino, D. Chen, and Q. Lu, "Nonlinear model for Galfenol cantilevered unimorphs considering full magnetoelastic coupling," *Journal of Intelligent Material Systems and Structures* **25**(2), pp. 187–203, 2014.